ARTICLE

Building blocks for the chemistry of perfluorinated alkoxyaluminates $[Al\{OC(CF_3)_3\}_4]^-$: simplified preparation and characterization of Li^+–Cs^+, Ag^+, NH_4^+, $N_2H_5^+$ and $N_2H_7^+$ salts†

Received 00th January 20xx,
Accepted 00th January 20xx

DOI: 10.1039/x0xx00000x

Przemysław J. Malinowski,[a]* Tomasz Jaroń,[a]* Małgorzata Domańska,[b] John M. Slattery,[c] Gustavo Santiso-Quinones,[d] Manuel Schmitt,[e] and Ingo Krossing[e]

Advanced weakly coordinating anions (WCAs) significantly facilitate synthesis of various exotic chemical compounds and novel, potentially useful materials. One of such anions – $[Al\{OC(CF_3)_3\}_4]^-$, denoted $[Al(OR^F)_4]^-$, appears particularly convenient, as it can be easily prepared from the commercially available alanates and $HOC(CF_3)_3$. Here we present a thorough characterization of a series of solvent-free $M[Al(OR^F)_4]$ salts, M = Li–Cs, Ag, NH_4, N_2H_5 and N_2H_7, and related compounds of monovalent cations, which are crucial starting materials for further work with these species. Notably, the corresponding synthetic protocols are updated by an improved method for fast, facile and easily scalable synthesis of $Li[Al(OR^F)_4]$, which remains the most useful primary source of the anion. The physico-chemical properties of these salts including crystal structures, thermal stability by TG/DSC, vibrational spectra as well as solubility are discussed in a systematic fashion.

Introduction

An extensive work on novel cationic complexes has been clearly facilitated by large developments in the field of progressively more advanced weakly coordinating anions (WCAs). Thanks to their properties like high robustness and weak basicity it was possible to obtain numerous compounds containing exotic cations, which includes noble gas complexes,[1] novel homopolyatomic cations like $[P_9]^+$,[2] complexes with atypical ligands, like $Fe(CO)_5$ [3,4] or N_2O,[5] silylium cations,[6] carbocationic species,[7] to mention just a few.[8,9] Some of these have shown good or unexpected catalytic activity,[10–14] the others can be potentially useful as electrolytes for batteries[15–17] or as convenient synthons towards materials like borohydrides, derivatives of ammonia borane or highly oxidizing compounds.[18–22]

Recently, significant advancements in the field of syntheses of two important types of WCA – fluorinated arylborates ($[B(Ar^F)_4]^-$, Ar^F = C_6H_3-3,5-$(CF_3)_2$)[23] and the parent carborane $[CB_{11}H_{12}]^-$ [24] were published in this journal. Along these lines we focus here on the most important WCA representative of the (per)fluorinated alkoxyaluminates, namely $[Al\{OC(CF_3)_3\}_4]^-$ (further denoted as $[Al(OR^F)_4]^-$). It is one of the least basic and least coordinating anions, surpassing the most advanced halogenated carboranes in this aspect (although not in the robustness).[25–28] At the same time, $[Al(OR^F)_4]^-$ is available in a multigram scale as Li salt at a reasonable price (*ca.* 2–3 EUR/g). While this anion reveals very high usefulness and we are aware of *ca.* 50 scientific groups worldwide using it, the data concerning its simplest and relatively accessible salts with the monovalent cations, $M^I[Al(OR^F)_4]$, where M=Li–Cs, NH_4, Ag, Tl or NO, should clearly be augmented. The synthetic protocols, NMR and vibrational spectra, as well as crystal structures of Li^+,[29] Cs^+,[30] Ag^+,[31] Tl^+[32,33] and NO^+,[34] are published at scattered places, while quite a few data is still missing. This motivated us to conduct the current systematic study concerning a series of $M[Al(OR^F)_4]$ salts, to support their further utilization.

The synthetic part of the work includes an overview and evaluation of synthetic protocols for M = Li^+-Cs^+, Ag^+, NH_4^+, $N_2H_5^+$ with particularly important being the one-pot synthesis of highly pure $Li[Al(OR^F)_4]$, starting directly from the commercially available precursors without the need of their purification. The analytical details concerning the obtained salts are presented including their vibrational spectra (FTIR and Raman), powder X-ray diffraction patterns and thermal decomposition data. We discuss the crystal structures of the solvent-free salts $M[Al(OR^F)_4]$ for M = Li–Cs (in the case of Li more accurate than recently published[29]) as well as the nitrogen-based cations like NH_4^+, $N_2H_5^+$ and $N_2H_7^+$. Owing to the high importance of the F-bridged anion presented in recent papers,[35–38] we also include the first crystal structures of the solvent-free M(I) (M = Ag, Cu) salts with the $[\{(CF_3)_3CO\}_3Al\text{-}F\text{-}Al\{OC(CF_3)_3\}_3]^-$ anion – a larger

[a] Centre of New Technologies, University of Warsaw, Banacha 2c, 02-097 Warsaw, Poland.
[b] Faculty of Physics, University of Warsaw, Pasteura 5,02-093 Warsaw, Poland.
[c] Department of Chemistry, University of York, Heslington, York YO10 5DD, United Kingdom.
[d] Crystallise! AG, Grabenstrasse 11a, 8952, Schlieren, Switzerland.
[e] Institut für Anorganische und Analytische Chemie and Freiburger Material-forschungszentrum (FMF), Universität Freiburg, Albertstr. 21, 79104 Freiburg, Germany.
* *Correspondence to malin@cent.uw.edu.pl and t.jaron@cent.uw.edu.pl*
†Electronic Supplementary Information (ESI) available: experimental details, crystallographic data, supplementary figures and NMR spectra, details to the quantum chemical calculations. See DOI: 10.1039/x0xx00000x

and more robust relative of $[Al(OR^F)_4]^-$, further denoted as [***alfal***]$^-$.

Results and discussion

Synthetic procedures

In this section we present a general discussion, while the technical details of the synthetic procedures are described in the **ESI**.

Li[Al(OR^F)$_4$]: Most of the synthetic protocols for the commonly used salts of $[Al(OR^F)_4]^-$ anions utilize $Li[Al(OR^F)_4]$ as a convenient and readily accessible precursor. While this salt can be easily prepared in large quantities (>100 g batches) according to Eq. (1),[25] its purification from the unreacted $LiAlH_4$ was the major remaining problem. This is caused by poor solubility of the product in the commonly used solvents selected from those showing sufficiently weak basicity to ensure lack of permanent complexation to Li^+.[28]

$$LiAlH_4 + 4\ HOR^F \xrightarrow{hexane} Li[Al(OR^F)_4] + 2\ H_2\uparrow \quad (1)$$

The contamination is particularly problematic when the product is further reacted with easily reducible species like Ag^+ salts.

To get product free from the residual hydride the protocol described in the book chapter from Ref. 39 (details in ESI) has to be followed *very strictly*. Yet, this imposes additional purification procedures so that the average time to prepare a 100 g batch of pure $Li[Al(OR^F)_4]$ takes at least three days for an experienced worker with the necessary laboratory setup. Thus, if the procedure is not followed strictly enough, trace amounts of hydride can still be present in the product, which is hard to detect using standard tests recommended earlier.[28]

During our research we have designed a readily available setup in which pure $Li[Al(OR^F)_4]$ can be synthesized in an efficient (yield >97%) and fast (few hours for 100 g batch), one-pot process using commercially available materials **without** the need of purification or drying. It was possible thanks to our observation that $Li[Al(OR^F)_4]$ is very well soluble in perfluorinated hydrocarbons (*ca.* 0.3 mol L^{-1}). Thus we have developed a simple apparatus made from standard laboratory glassware (*c.f.* ESI), in which reaction (1) is conducted on a glass extraction frit with *iso*-C_6F_{14} as a solvent, the cheapest of all perfluorinated solvents. Only the targeted compound is soluble in C_6F_{14} making it possible to separate unreacted $LiAlH_4$ as well as other ionic impurities like Li complexes with siloxanes[40] or water molecules. For more details please refer to the ESI.

The purity of the final product has been checked using powder diffraction and spectroscopic methods (IR, NMR), revealing no impurities detectable with these techniques, *i.e.* other crystalline phases or compounds with remaining Al–H bonds.

M[Al(OR^F)$_4$], M = Na–Cs: $Na[Al(OR^F)_4]$ and $K[Al(OR^F)_4]$ can be prepared in the reactions analogous to (1), *i.e. via* alcoholysis of the corresponding alanates, which are either available commercially ($NaAlH_4$), or can be easily synthesized ($KAlH_4$).[18,41] However, for K^+–Cs^+ a metathetic ion exchange between $Li[Al(OR^F)_4]$ and the appropriate halide, preferably chloride, Eq. 2, conducted in DCM and with subsequent extraction of $M[Al(OR^F)_4]$ with this solvent is the most convenient approach.

$$MX + Li[Al(OR^F)_4] \rightarrow LiCl + M[Al(OR^F)_4] \quad (2)$$

(X=Cl for M = K–Cs and X=F for M=Ag)

For the Na salt we would recommend reaction (1) with $NaAlH_4$ as the method of choice, since metathesis (2) starting from $Li[Al(OR^F)_4]$ either in CH_2Cl_2 or in C_6F_{14}, yields a poor conversion rate even upon prolonged reaction times. However, the ease of the conversion of Eq. (2) increases down the periodic table. While an overnight ultrasound-enhanced reaction in DCM for M = K leads to mere 40%, the yield rises to *ca.* 60% for Rb and to *ca.* 80 % for Cs. Despite moderate yield for K, we still recommend this method to conveniently prepare the pure salt. Higher conversion rates for K and Rb can be achieved, if the reactions are induced mechanochemically using a high-energy ball mill (*c.f.* ESI). An 80% yield for $K[Al(OR^F)_4]$ is reached after mere 30 minutes of milling. However, highly dispersed LiCl and MCl may form, which are difficult to separate completely from $M[Al(OR^F)_4]$ even by filtering the obtained suspension in DCM through a fine P4 frit.‡ More details on this can be found in ESI.

NH$_4$[Al(OR^F)$_4$] and N$_2$H$_5$[Al(OR^F)$_4$] can be prepared from $Li[Al(OR^F)_4]$ and NH_4^+ or $N_2H_5^+$ chlorides, respectively, using the adjusted metathesis Eq. (2). However, solely for the reaction mediated by DCM with ultrasonic enhancement we were able to obtain pure $NH_4[Al(OR^F)_4]$, and only when the excess of $[NH_4]Cl$ did not exceed *ca.* 150 mol-%. Application of the mechano-chemical approach or large excess of $[NH_4]Cl$ in the solvent-mediated process resulted in a slightly contaminated product as observed in the powder diffractogram, *cf.* Fig. S9. The contamination was further identified as $N_2H_7[Al(OR^F)_4]$ on the basis of its crystal structure solved from single crystal X-ray diffraction data, and we have not attempted to characterize it fully. However, our DFT calculations (B3LYP/def2-TZVP/D3BJ) show that the energetics of reaction (3) can explain the formation of $N_2H_7^+$ in the system. Indeed, reaction (3),

$$NH_4^+{}_{(g)} + [NH_4]Cl_{(g)} \rightarrow N_2H_7^+{}_{(g)} + HCl_{(g)} \quad (3)$$

for species in the gas phase is thermodynamically favorable with $\Delta_r G = -89$ kJ mol^{-1}. Our results show that in a very weakly basic environment provided by CH_2Cl_2 and $[Al(OR^F)_4]^-$ (pseudo gas conditions), even the NH_4^+ cation can become sufficiently acidic to compete with the molecular HCl in bonding to NH_3.[8]

Ag[Al(OR^F)$_4$]: For M = Ag, we have realized that liquid SO_2 is the best solvent for performing reaction (2), though in the previous study C_6F_{14} was also used. Using SO_2 yields a colorless solution of the Ag salt, while in the analogous route with DCM the ***solution*** is beige to brown due to contamination with the Ag^0 or AgCl particles, probably as a result of slow decomposition of CH_2Cl_2 by Ag^+ or due to the reaction with trace $LiAlH_4$ or silicon grease. This may be the case, even if pure $Li[Al(OR^F)_4]$, *i.e.* free from the Al–H contaminations, has been used. These Ag^0 and AgCl contaminations are responsible for very high fluorescence making it impossible to measure Raman spectrum of so obtained $Ag[Al(OR^F)_4]$,[28] which is not an issue when using SO_2 as a reaction medium.[35] This observation confirms the purity of the obtained material. Complete conversion of $Li[Al(OR^F)_4]$ to

$Ag[Al(OR^F)_4]$ is also possible in C_6F_{14},[31] but subsequent extraction of the product is tedious due to the inferior solubility. For completeness, we would like to mention our recently reported method[5] for the preparation of $[Al(OR^F)_4]^-$ salts by metathesis of the corresponding $[AlCl_4]^-$ salt with the known tetrameric alkoxide $[LiOC(CF_3)_3]_4$.[42]

Fluoride-bridged salts of Cu and Ag: Cu[***alfal***] forms during heating the suspension of $Cu[Al(OR^F)_4]$ in degassed C_6F_{14} to about 40–45°C for 30 minutes.§ Contrary to $Cu[Al(OR^F)_4]$, Cu[***alfal***] is well soluble in C_6F_{14}, from which its crystals can be grown. However, attempts to isolate the product on larger scale are difficult, since the crystals tend to cover with a sticky layer probably formed by other products of decomposition of $Cu[Al(OR^F)_4]$. The solvent-free Ag[***alfal***] compound prepared according to Ref. 35 crystallizes from C_6F_6 solution.

Crystal and molecular structures

Among the non-solvated salts containing the $[Al(OR^F)_4]^-$ anion, only the structures of $Li[Al(OR^F)_4]$ (measured at 123 K),[29] $Cs[Al(OR^F)_4]$ (*Cc*, measured at 223 K),[30] $Tl[Al(OR^F)_4]$,[32,33] $Ag[Al(OR^F)_4]$[31] and $NO[Al(OR^F)_4]$[34] have been reported. Here we present the structures of the $M[Al(OR^F)_4]$ crystals, M = Li–Cs, measured at 100 K (except for M = Na). The crystal structure of $Li[Al(OR^F)_4]$ has been re-determined with anisotropic refinement and accurate resolution of disorder. For $Cs[Al(OR^F)_4]$ a different polymorph of is described. The details of the crystal structures of the $M[Al(OR^F)_4]$ salts are listed in Table S2 (ESI).

$M[Al(OR^F)_4]$, M = Li–Cs. Although all these compounds are formally ionic salts, the specific coordination mode in $M[Al(OR^F)_4]$ strictly depends on the size of the cation. For Li, Na and Ag[31] the metal cations remain stuck in the $[Al(OR^F)_4]^-$ anion, forming an ion pair with two relatively short bonds to the oxygen atoms and three M–F bonds. This causes significant deformation of the $[Al(OR^F)_4]^-$ anion. A similar bonding pattern has been reported for a few known solvated Ag compounds like $Ag(SO_2)[Al(OR^F)_4]$[43] or $Ag(C_6H_4(CF_3)_2)[Al(OR^F)_4]$.[25]

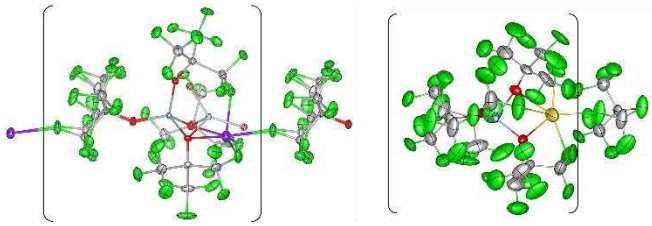

Figure 1. The view of $Li[Al(OR^F)_4]$ (left) and $Na[Al(OR^F)_4]$ (right) units (in parentheses) in the crystal structure shown together with the M-F bonds to adjacent units forming a 1D chain. C – grey, F – green, Li – purple, Na –yellow, O – red, Al – blue; O and Al atoms from the opposite orientation of the anion in $Li[Al(OR^F)_4]$ are pink and pale blue. Thermal ellipsoids shown at 50% probability level.

The M–F contacts to the adjacent anions are weak, *e.g.* for M = Li this distance is equal to 2.186(9) Å, which is larger than the sum of the ionic radii of F^- and Li^+ at 1.90 Å (c.n. 4) or 2.09 Å (c.n. 6).[44] For comparison, within ion pairs the Li–O bonds are shorter, *e.g.* *d*(Li–O)= 2.057(5) Å, but *d*(Li–F) are in the same range as above: 2.148(5) Å, 2.151(5) Å and 2.251(5) Å. These separations are much longer than those found in classical salts like $Li[BF_4]$, where *d*(Li–F) = 1.846(5) Å (at 200 K)[45] or $Li[SO_3CF_3]$, where *d*(Li–O) is in the range 1.87–1.99 Å (at 173 K).[46]

In $Na[Al(OR^F)_4]$ *d*(Na–O) and *d*(Na–F) remain within 2.46(1)–2.61(1) Å and 2.32(1)–2.68(1) Å, respectively, *i.e.* slightly shorter than in $Ag[Al(OR^F)_4]$[31], which is expected on the basis of the relative ionic radii. Interestingly, the shortest Na–F distance links the adjacent anion, what may explain the poorer solubility of $Na[Al(OR^F)_4]$ in the perfluorinated solvents.

The tight ion pairs present in the crystal structures of Li, Na and Ag salts form 1D infinite antiparallel $(M[Al(OR^F)_4])_\infty$ chains linked by M–F contacts (Figure 1). Since the interactions between these chains are limited to weak electrostatic contacts between the F atoms, the energy difference between the parallel and the antiparallel arrangement must be very low. Indeed, *ca.* 2% of the chains in $Li[Al(OR^F)_4]$ and $Na[Al(OR^F)_4]$ and 4% in $Ag[Al(OR^F)_4]$ are aligned contrary to the main direction, which is visible as a disorder of the orientation of the $M[Al(OR^F)_4]$ moieties (Fig. S15). This feature has not been detected in the previous work reporting the crystal structure of $Li[Al(OR^F)_4]$,[29] probably due to slightly inferior dataset collected. However, it can have a significant impact on the quality of the refined model as we have experienced during the structure refinement of $Ag[Al(OR^F)_4]$.[31] Assuming that the two disordered orientations of the structures represent the thermodynamic minima, an energy difference of *ca.* 10 kJ mol^{-1} for Li and Na and *ca.* 8 kJ mol^{-1} for the Ag salt is expected between them according to the Boltzmann distribution.

With the larger cations, *i.e.* K^+, Rb^+ (isostructural to Tl^+),[33] Cs^+ as well as the N–H based cations, the situation is different. These cations are located between the anions, forming truly ionic structures with no M–O contact present. Each cation is surrounded by four virtually undistorted $[Al(OR^F)_4]^-$ anions with [MAl] sublattices adopting slightly deformed ZnS structures for NH_4, Rb and Cs (Fig. S13). For potassium this sublattice is more complex not belonging to any simple structure type (see Fig. S12). The relationship between the previously reported *Cc* structure (223 K)[30] and the low-symmetry 100 K-polymorph of $Cs[Al(OR^F)_4]$ presented in this study, is clearly visible analyzing the [CsAl] sublattice. In the former structure Cs and Al are linearly stacked in the [010] direction, while the latter reveals slight modulation of this sublattice, Fig. S14. The cations in $M[Al(OR^F)_4]$ are coordinated by 10 to 12 F atoms, ranging between 2.667(1)–3.140(2) Å for K^+ (ionic radii sum: 2.71 Å), 2.867(3) Å–3.468(4) Å for Rb^+ (ionic radii sum: 2.85 Å) and 3.033(9)–3.653(10) Å for Cs^+ (ionic radii sum: 3.00 Å).

In each case, the bond valence sum[47] for M is slightly below 1 (around 0.95),§§ indicating the possibility of weak underbonding in these species, which enhances their coordinative abilities. Indeed, the facile crystal growths of $Cs(C_6H_5CH_3)[Al(OR^F)_4]$ incorporating toluene underlines this speculation, *cf.* Fig. S17 and Table S3 in the ESI.

Salts of N–H cations. Ammonium and hydrazinium salts crystallize in *P*1 unit cells isostructural with $Rb[Al(OR^F)_4]$. Although it is not possible to determine the exact positions of the hydrogen atoms in $[NH_4]^+$ and $[N_2H_5]^+$, the shortest N–F distances at *ca.* 2.9 Å suggest that N–H···F_3C hydrogen bonds form.[48] The analysis of IR spectra of the ammonium salt

presented below gives further evidence to that notion. It has to be underlined that the CF_3 group is a very poor H-bond acceptor and the existence of N–H···F_3C hydrogen bond was experimentally proven only in 2013.[49] Therefore, these two compounds may serve as convenient models for further study in this area.

$N_2H_7[Al(OR^F)_4]$ contains the $[NH_4^+{\cdot}NH_3]$ ion, which is the simplest member of the family of ammine-ammonium complexes, *e.g.* $[NH_4(NH_3)_x]^+$ (with *x* varying from 1 up to 10 in the gas phase[50]). A few of the salts composed of $[N_2H_7]^+$ cations have been characterized structurally, which include $[N_2H_7][CH_3COO]$,[51] $[N_2H_7]I$,[52] $[N_2H_7]F$,[53] or the compounds containing larger phenolic anions.[54] The ion centers in $[N_2H_7][Al(OR^F)_4]$ form a distorted NaCl-type lattice. The N–N distances found (2.674(5)–2.700(5) Å) are similar to those reported for the $[N_2H_7]^+$ salts mentioned above. The nearest N–F distances of *ca.* 2.9 Å again suggest the presence of weak N–H···F_3C hydrogen bonds.

M[alfal], M = Ag(I) and Cu(I). These compounds form tight ion pairs in the solid state, similarly to the $M[Al(OR^F)_4]$ salts of M = Li, Na and Ag. However, contrary to the latter, no M–F or M–O interactions to neighboring $[alfal]^-$ are present in the crystal structures of M[***alfal***] and M form bonds *solely* the anion in which it is stuck. These Ag(I) and Cu(I) compounds are not isostructural and incorporate slightly different packing and bonding fashion within the M[***alfal***] structural units, Figure 2.

The coordination of silver is a distorted trigonal prism with three oxygen atoms residing on the bottom and three fluorine atoms at the top of the prism. Two of the Ag–O distances resemble those in $Ag[Al(OR^F)_4]$, while the third is significantly longer. There are only three Ag–F bonds in the structure of Ag[***alfal***], while two of them are rather short as for CF_3···Ag interactions. In the Cu[***alfal***] ion-pair the cation is coordinated only by two oxygen and two fluorine atoms, also at fairly short distances of 2.014(5)–1.975(6) Å for O and 2.343(5)–2.394(5) Å for F. The coordination sphere is irregular and could be described as highly distorted square or tetrahedron. The coordination of Ag or Cu to oxygen atoms results in bending of the Al–F–Al bridge to around 165° and elongation of the Al–O bonds with O atoms coordinating M^+. Despite the short M–O and M–F contacts, the bond valence sums for Ag^+ and Cu^+ remain close to 0.8. Such significant underbonding indicates strong coordinative unsaturation of the cations.

Vibrational spectroscopy

The measured MIR spectra of the salts of $[Al(OR^F)_4]^-$ are dominated by the absorption bands related to the vibrations of the anion, with very well visible characteristic peaks around

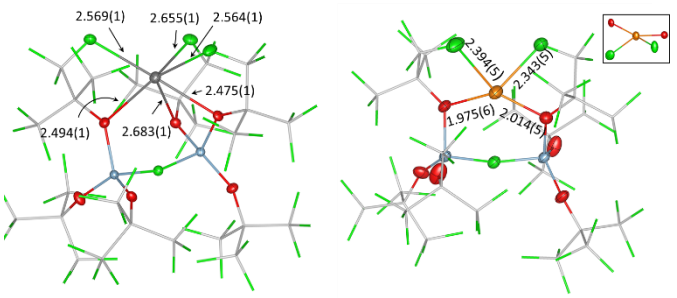

Figure 2. Views of the Ag[***alfal***](left) and Cu[***alfal***] (right) molecular structures observed in their crystals with metal-O and metal-F bond lengths given (in Å). The inset shows a different orientation of the Cu coordination sphere. To keep the figure legible only thermal ellipsoids (50% probability level) for the O_3Al-F-AlO_3 fragments are shown together with the F atoms bonding to Ag or Cu.

727 cm^{-1}, 961–976 cm^{-1} and a series of very strong bands in the region of 1100–1400 cm^{-1}, Figure 3 and Table S1 (ESI). The spectra of the salts containing virtually undistorted anions, M = K–Cs, NH_4 and NO, remind to those of the tetraalkylammonium salts besides the vibrations of the NR_4^+ cations.[55]

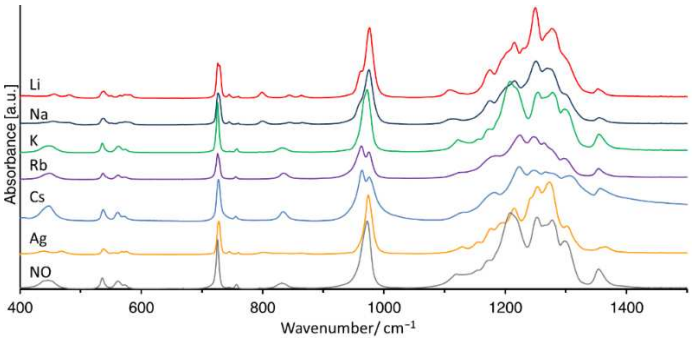

Figure 3. The FTIR spectra (measured on ATR module) of a series of $M[Al(OR^F)_4]$ salts, M = Li–Cs, Ag. For comparison, also the $NO^+[Al(OR^F)_4]^-$ spectrum is included.[34]

As it already has been discussed for M = Li and Ag, lowering of the anion symmetry due to its distortion, results in splitting of numerous absorption bands, which is observed for M = Li, Na and Ag.[55] A few of these split bands, like those around 745 cm^{-1} or 799 cm^{-1}, are only Raman active modes in the compounds containing anions of nearly ideal S_4 symmetry. In the case of Rb and Cs salts, the bands around 963 cm^{-1} are clearly separated from those at *ca.* 975 cm^{-1}, while for the other compounds only shoulders (M = Li, Na, K, NH_4, NR_4^+), or a single band (M = Ag) are present in this wavenumber range.

Raman spectra of $M[Al(OR^F)_4]$ (*c.f.* ESI) are almost identical and contain only several weak bands from $[Al(OR^F)_4]^-$. Various types of bonding (via O or F atoms) do not influence these spectra to any significant level.

The salts containing NH_4^+ and $N_2H_5^+$ cations, aside of the modes characteristic for $[Al(OR^F)_4]^-$, reveal the bands typical for these N–H species (see Figure 4 and Table S1). *ν*(NH) in $NH_4[Al(OR^F)_4]$ is found at 3324 cm^{-1}, with the two shoulders at 3236 cm^{-1} and 3434 cm^{-1}. In $N_2H_5[Al(OR^F)_4]$ these bands are found in the range of 3186–3413 cm^{-1} with the strongest band at 3300 cm^{-1}. Both ν(NH) and δ(HNH) for ammonium salt are very broad what is partly the consequence of disorder which is common to the

compounds with $[Al(OR^F)_4]^-$. The shape of these bands is also influenced by weak N–H···F_3C hydrogen bonds,[56] indicated by the observed N–F distances.

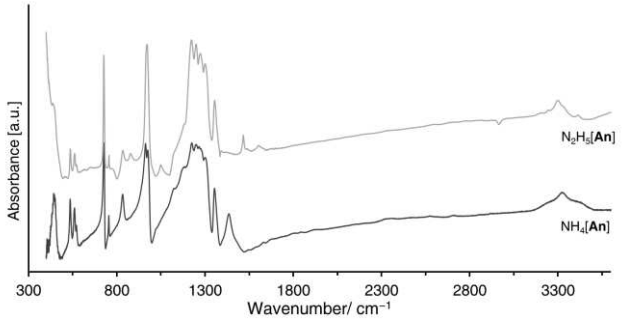

Figure 4. IR spectra of $NH_4[Al(OR^F)_4]$(grey) and $N_2H_5[Al(OR^F)_4]$ (black).

Solubility

Due to very low lattice energy and its interplay with the solvation enthalpies of ions, the WCA salts are soluble even in solvents of low solvation ability, as characterized by a small dielectric constant and the absence of clear donor atoms (O, N). This is not the case for the typical inorganic salts. While the solubility of a few salts containing the $[Al(OR^F)_4]^-$ anion has been mentioned in several papers, virtually no quantitative data were reported besides those concerning the tetraalkylammonium salts.[55] We have quantitatively tested and evaluated the solubility of selected $M[Al(OR^F)_4]$ salts in three solvents: dichloromethane, trifluorotoluene ($C_6H_5CF_3$), and perfluorohexane (mixture of isomers, mostly *iso*-). The two former solvents are moderately polar with dielectric constants (ε_r) around 9, promoting dissociation of the salts of moderate lattice energy, the third is a fluorous solvent of very low polarity (ε_r = 1.69 for *n*-C_6F_{14}), which facilitates solubility of the neutral, highly fluorinated compounds. As expected, the solubility of the examined salts strongly depends on the character of the M^+ cations and is clearly related to the crystal structure of the salts, Table 1.

Table 1. Solubility in [mol L^{-1}] of the selected $M[Al(OR^F)_4]$ salts in three solvents. X denotes very poor solubility, which was difficult to measure reliably. Note that due to the high molecular masses 0.01 mol L^{-1} correspond to ca. 10 g L^{-1}. $T \approx 25$ °C.

Solvent	Li	Na	Rb	Cs	NH_4	Ag
CH_2Cl_2	X	0.002	0.02	0.03	0.035	Very high
$C_6H_5CF_3$	0.037	0.009	0.024	–	0.014	> 0.36
iso-C_6F_{14}	0.30	0.003	X	X	X	0.003
SO_2	well soluble; no quantitative data					

The true salts containing larger cations like NH_4, Rb, Cs are relatively well soluble in dichloromethane and in $C_6H_5CF_3$. The solubility of $NH_4[Al(OR^F)_4]$ and $Cs[Al(OR^F)_4]$ in CH_2Cl_2 is similar to that of $[NBu_4][Al(OR^F)_4]$ (*ca.* 0.04 mol L^{-1}).[55] However, these salts, due to their clearly ionic character, are not soluble in the perfluorinated solvents, which do not enable electrolytic dissociation. The situation is reversed for the ion-pairs, *i.e.* $M[Al(OR^F)_4]$ with M = Li, Na and Ag, but also Ag[***alfal***] and Cu[***alfal***]. In this case, the adjacent ion pairs interact only due to weak M–F bonds or via even weaker F···F dispersive attractions, which can be equally well formed with the molecules of a perfluorinated solvent. As a result $Li[Al(OR^F)_4]$ is soluble in C_6F_{14} to an extent allowing for its purification *via* extraction using this solvent. While only traces of $Li[Al(OR^F)_4]$ dissolve in CH_2Cl_2 it is still sufficient for performing ion metathesis reactions in this solvent.[18–22]

The ease of solvation of the relatively soft Ag^+ cations (that form bonds of much more covalent character than Na or Li) by dichloromethane molecules renders $Ag[Al(OR^F)_4]$ very well soluble in this solvent. Though without quantitative determination, we have observed that many solvent-free $M[Al(OR^F)_4]$ salts, particularly with M = Li – K, NH_4, N_2H_5 and Ag, are well soluble in SO_2, what broadens the scope of weakly basic and robust solvents usable with these compounds.

Thermal decomposition

Thermal decomposition of the $M[Al(OR^F)_4]$ salts for M=Li–Cs, Ag, NH_4 and N_2H_5, as well as NO (added for the sake of completeness as this is also an important reagent[34]), has been investigated using TGA/DSC coupled with temperature-resolved mass spectrometry, Fig. 5–7, Table 2. All these compounds decompose in complicated multistep processes, which are predominantly endothermic. Due to such complexity the detailed investigation of their mechanisms remains beyond the scope of the present study. The salts of alkali metals reveal a clear trend in thermal stability, which strongly increases (up to *ca.* 290°C for Cs) with decreasing Lewis acidity and increasing size of the M^+ cation. Apparently, ion pairing observed in the crystal structures is another factor facilitating thermal decomposition. Based on the previous reports and the recorded mass spectra of the evolving gases, octafluoroisobutylene epoxide, C_4OF_8, is the most probable volatile decomposition product.[28,§§§] The mass of the decomposition residue remains below the expected value for $MF+AlF_3$ for all the alkali metal salts. For $Li[Al(OR^F)_4]$ two endothermic DSC peaks observed at 46°C and 54°C without simultaneous mass loss apparently correspond to polymorphic transitions.

Table 2. Summary of TGA and DSC results for $M[Al(OR^F)_4]$, M = Li – Cs, NH_4, Ag, NO. T_{DSCMIN} – temperature of the first DSC peak of thermal decomposition; m_{RES} – residual mass at the end of experiment.

M	Mass loss onset [°C]	T_{DSCMIN} [°C]	m_{res} [%]
Li	105	156	1.6
Na	175	236	1.9
K	250	253	2.9
Rb	275	276	4.1
Cs	285	288	12.0
Ag	75	96	15.3
NH_4	120	143	1.7
N_2H_5	133	159	1.2
NO	98	132	9.6

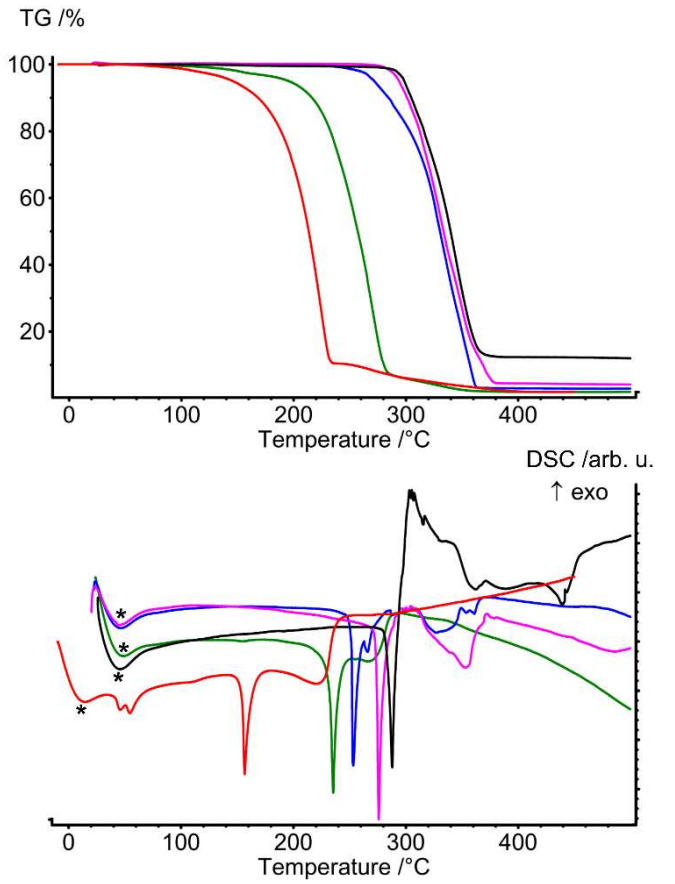

Figure 5. TGA (top) and DSC (bottom) plots of M[Al(OR^F)$_4$], M = Li (red), Na (green), K (blue), Rb (purple), Cs (black). The artifacts on the DSC curves have been marked with asterisks (*). The measurement for M=Li has been performed starting from −10 °C, while the others start from RT. All measurements were performed at a 5 °C min^{-1} heating rate.

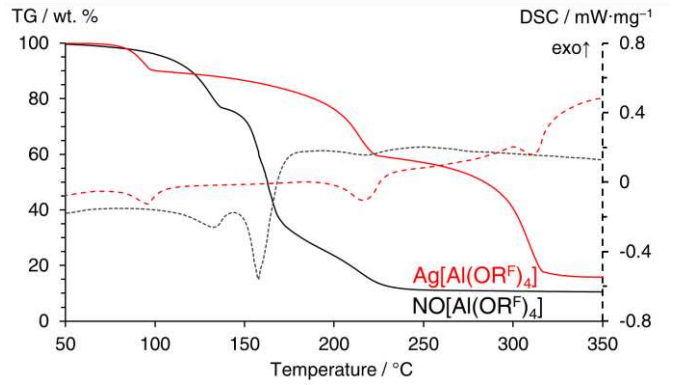

Figure 6. TGA (full lines) and DSC (dashed lines) plots of Ag[Al(OR^F)$_4$] (red) and NO[Al(OR^F)$_4$] (black) heated at the rate of 5 °C min^{-1}.

For the cations of more covalent and oxidizing character, i.e. Ag^+, Cu^+ [5] and NO^+ the decomposition starts already below 100 °C. Our results indicate that the thermal stability of Ag[Al(OR^F)$_4$] is in fact slightly lower than reported previously, where 97–100°C was given as melting and decomposition temperature.[25] This may be due to more sensitive analytical technique used in the present study.

Thermal decomposition of the nitrosyl salt starts already at 65°C, where signals of the anion decomposition are visible in the MS spectra. There are three distinguishable decomposition steps present and the remaining mass at 250°C is *ca.* 10 wt.%, what corresponds well to the expected amount of AlF_3. However, MS spectra show no signs of NO (m/z = 30), and the solid residue is highly porous and bulky, which makes the fate of NO^+ in the process unclear.

The stability of NH_4 and N_2H_5 salts is significantly lower than that of the alkaline metal salts, what is a common trend for simple inorganic salts with the anions like sulfates of phosphates. Both start to decompose around 120°C and proceeds until 200°C or 225°C, respectively leaving less than 2 wt.% of initial mass. MS spectra show the presence of perfluorinated compounds as well as NH_3.

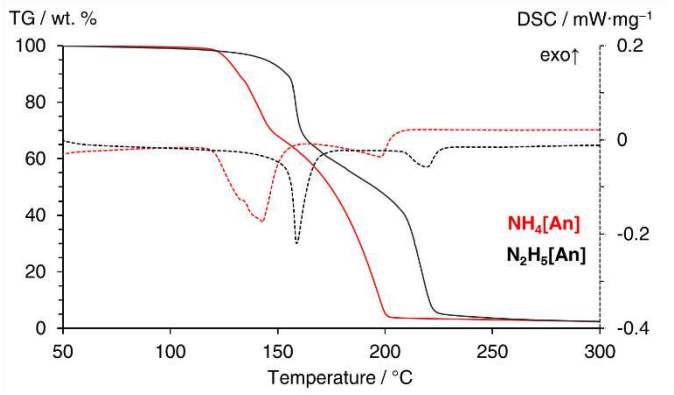

Figure 7. TG (solid) and DSC (dashed) curves for NH$_4$[Al(OR^F)$_4$] (red) and N$_2$H$_5$[Al(OR^F)$_4$] (black) heated at the rate of 5 °C min^{-1}.

Conclusions

The salts of $[Al(OR^F)_4]^-$ containing monovalent cations, M^+, are convenient starting materials for most of the processes in which these weakly coordinating anions are used. The paper presents an overview of convenient methods for their preparation using accessible laboratory setup and several routes of synthesis. Notably, we have developed a one-step and easily scalable synthetic approach towards the most important of the starting salts - Li[Al(OR^F)$_4$]. Physicochemical properties in the series of M = Li–Cs, Ag, NH_4, N_2H_5 strongly depend on the character of the cation but follow clear trends. Larger cations form true salts with thermal stability up to almost 300°C and high solubility in weakly coordinating, yet polar solvents. By contrast, the ion-paired molecular M[Al(OR^F)$_4$] with M = Li, Na or Ag dissolve in perfluorocarbons, a feature rarely encountered in pseudo-binary salts. As shown in this paper, it can be exploited to design elegant synthetic procedures or, as it has been already shown in several recent works,[5,31] to extend chemistry to unusual compounds. The characteristics of the presented set of salts will enable further development of chemistry of unusual and potentially useful complexes.

Experimental and Method Section

All syntheses and manipulations were performed under inert atmosphere (5.0 Ar filled glovebox or vacuum line). Unless stated otherwise, all the solvents were dried with conventional laboratory methods prior to use. Extensive description of the experimental parts can be found in the **ESI**. CCDC entries # 1960194–1960199, 1960204–1960205, 1960207, 1960459 and 1960514 contain the supplementary crystallographic data for this paper. These data are provided free of charge by The Cambridge Crystallographic Data Centre.

Conflicts of interest

There are no conflicts to declare.

Acknowledgements

PJM is grateful for financial support from National Science Centre (UMO-2014/15/D/ST5/02580). TJ and MD appreciate the financial support from the Foundation for Polish Science (Homing Programme, agreement No. POIR.04.04.00-00-221F/16-00). The authors thank the Biopolymers Laboratory, Faculty of Physics, University of Warsaw, for the access to Agilent Supernova X-ray single-crystal diffractometer, co-financed by the European Union within the ERDF Project POIG.02.01.00-14-122/09.

Notes and references

‡ It has to be noted that the amount is not high. Salts MCl have highly symmetric unit cells what makes their reflexes clearly visible even at low concentration when mixed with less symmetric compounds with large unit cells.

§ note: $Cu[Al(OR^F)_4]$ is obtained in the mixture of AgI and Cu.[5]

§§ Bond valence parameters: R_0(K–F) = 1.992; R_0(Rb–F) = 2.16; R_0(Cs–F) = 2.33, B= 0.37. Taken from "Bond valence parameters" IUCr, dataset bvparm2016.cif available at https://www.iucr.org/resources/data/data-sets/bond-valence-parameters and retrieved on 05.06.2019.

§§§ The exact identity of the evolved gases is hard to determine as there are plenty of signals present in the mass spectra of limited resolution. However, the dominating peak at m/z = 69 points to the presence of CF_3 groups. Most probably the dominating gas evolved is C_4F_8O, as reported for this class of compounds (*cf.* [28]).

1 S. Seidel and K. Seppelt, *Science (80-.).*, 2000, **290**, 117–118.

2 T. Köchner, T. A. Engesser, H. Scherer, D. A. Plattner, A. Steffani and I. Krossing, *Angew. Chemie - Int. Ed.*, 2012, **51**, 6529–6531.

3 P. J. Malinowski and I. Krossing, *Angew. Chemie - Int. Ed.*, 2014, **53**, 13460–13462.

4 G. Wang, Y. S. Ceylan, T. R. Cundari and H. V. R. Dias, *J. Am. Chem. Soc.*, 2017, **139**, 14292–14301.

5 V. Zhuravlev and P. J. Malinowski, *Angew. Chemie Int. Ed.*, 2018, **57**, 11697–11700.

6 K. C. Kim, C. A. Reed, D. W. Elliott, L. J. Mueller, F. Tham, L. Lin and J. B. Lambert, *Science (80-.).*, 2002, **297**, 825–827.

7 M. Schorpp, S. Rein, S. Weber, H. Scherer and I. Krossing, *Chem. Commun.*, 2018, **54**, 10036–10039.

8 I. M. Riddlestone, A. Kraft, J. Schaefer and I. Krossing, *Angew. Chemie - Int. Ed.*, 2018, **57**, 13982–14024.

9 I. Krossing and I. Raabe, *Angew. Chemie Int. Ed.*, 2004, **43**, 2066–2090.

10 M. R. Lichtenthaler, A. Higelin, A. Kraft, S. Hughes, A. Steffani, D. A. Plattner, J. M. Slattery and I. Krossing, *Organometallics*, 2013, **32**, 6725–6735.

11 M. R. Lichtenthaler, S. Maurer, R. J. Mangan, F. Stahl, F. Mönkemeyer, J. Hamann and I. Krossing, *Chem. - A Eur. J.*, 2015, **21**, 157–165.

12 V. Volkis, H. Mei, R. K. Shoemaker and J. Michl, *J. Am. Chem. Soc.*, 2009, **131**, 3132–3133.

13 N. Klikovits, P. Knaack, D. Bomze, I. Krossing and R. Liska, *Polym. Chem.*, 2017, **8**, 4414–4421.

14 A. Peter, S. M. Fehr, V. Dybbert, D. Himmel, I. Lindner, E. Jacob, M. Ouda, A. Schaadt, R. J. White, H. Scherer and I. Krossing, *Angew. Chemie Int. Ed.*, 2018, **57**, 9461–9464.

15 J. T. Herb, C. A. Nist-Lund and C. B. Arnold, *ACS Energy Lett.*, 2016, **1**, 1227–1232.

16 Z. Zhao-Karger, M. E. Gil Bardaji, O. Fuhr and M. Fichtner, *J. Mater. Chem. A*, 2017, **5**, 10815–10820.

17 A. Shyamsunder, W. Beichel, P. Klose, Q. Pang, H. Scherer, A. Hoffmann, G. K. Murphy, I. Krossing and L. F. Nazar, *Angew. Chemie Int. Ed.*, 2017, **56**, 6192–6197.

18 T. Jaroń, P. A. Orłowski, W. Wegner, K. J. Fijałkowski, P. J. Leszczyński and W. Grochala, *Angew. Chemie Int. Ed.*, 2015, **54**, 1236–1239.

19 T. Jaroń, W. Wegner, K. J. Fijałkowski, P. J. Leszczyński and W. Grochala, *Chem. - A Eur. J.*, 2015, **21**, 5689–5692.

20 A. Starobrat, M. J. Tyszkiewicz, W. Wegner, D. Pancerz, P. A. Orłowski, P. J. Leszczyński, K. J. Fijalkowski, T. Jaroń and W. Grochala, *Dalt. Trans.*, 2015, **44**, 19469–19477.

21 R. Owarzany, K. J. Fijalkowski, T. Jaroń, P. J. Leszczyński, Ł. Dobrzycki, M. K. Cyrański and W. Grochala, *Inorg. Chem.*, 2016, **55**, 37–45.

22 T. E. Gilewski, P. J. Leszczyński, A. Budzianowski, Z. Mazej, A. Grzelak, T. Jaroń and W. Grochala, *Dalt. Trans.*, 2016, **45**, 18202–18207.

23 A. J. Martínez-Martínez and A. S. Weller, *Dalt. Trans.*, 2019, **48**, 3551–3554.

24 L. Toom, A. Kütt and I. Leito, *Dalt. Trans.*, 2019, **48**, 7499–7502.

25 I. Krossing, *Chem. - A Eur. J.*, 2001, **7**, 490–502.

26 T. J. Barbarich, S. T. Handy, S. M. Miller, O. P. Anderson, P. A. Grieco and S. H. Strauss, *Organometallics*, 1996, **15**, 3776–3778.

27 S. M. Ivanova, B. G. Nolan, Y. Kobayashi, S. M. Miller, O. P. Anderson and S. H. Strauss, *Chem. - A Eur. J.*, 2001, **7**, 503–510.

28 I. Krossing and A. Reisinger, *Coord. Chem. Rev.*, 2006, **250**, 2721–2744.

29 X. Zheng, Z. Zhang, G. Tan and X. Wang, *Inorg. Chem.*, 2016, **55**, 1008–1010.

30 I. Krossing, H. Brands, R. Feuerhake and S. Koenig, *J. Fluor. Chem.*, 2001, **112**, 83–90.

31 P. J. Malinowski, D. Himmel and I. Krossing, *Angew. Chemie Int. Ed.*, 2016, **55**, 9259–9261.

32 M. Gonsior, I. Krossing and N. Mitzel, *Zeitschrift fur Anorg. und Allg. Chemie*, 2002, **628**, 1821–1830.

33 P. Weis, D. C. Röhner, R. Prediger, B. Butschke, H. Scherer, S. Weber and I. Krossing, *Chem. Sci.*, 2019, **10**, 10779–10788.

34 T. A. Engesser, C. Friedmann, A. Martens, D. Kratzert, P. J. Malinowski and I. Krossing, *Chem. - A Eur. J.*, 2016, **22**, 15085–15094.

35 A. Martens, P. Weis, M. C. Krummer, M. Kreuzer, A. Meierhöfer, S. C. Meier, J. Bohnenberger, H. Scherer, I. Riddlestone and I. Krossing, *Chem. Sci.*, 2018, **9**, 7058–7068.

36 J. Bohnenberger, B. Derstine, M. Daub and I. Krossing, *Angew. Chemie Int. Ed.*, 2019, **58**, 9586–9589.

37 J. Bohnenberger, W. Feuerstein, D. Himmel, M. Daub, F. Breher and I. Krossing, *Nat. Commun.*, 2019, **10**, 624.

38 A. Martens, M. Kreuzer, A. Ripp, M. Schneider, D. Himmel, H. Scherer and I. Krossing, *Chem. Sci.*, 2019, **10**, 2821–2829.

39 I. K. I. Raabe, A. Reisinger, in *Experiments in Green and Sustainable Chemistry (Eds. H. W. Roesky, D. K. Kennepohl)*, Wiley-VCH, Weinheim, 2009, pp. 131–144.

40 T. S. Cameron, A. Decken, I. Krossing, J. Passmore, J. M. Rautiainen, X. Wang and X. Zeng, *Inorg. Chem.*, 2013, **52**, 3113–3126.

41 J. A. Dilts and E. C. Ashby, *Inorg. Chem.*, 1972, **11**, 1230–1236.

42 I. Raabe, K. Wagner, G. Santiso-Quiñones and I. Krossing, *Zeitschrift für Anorg. und Allg. Chemie*, 2009, **635**, 513–517.

43 A. Decken, C. Knapp, G. B. Nikiforov, J. Passmore, J. M. Rautiainen, X. Wang and X. Zeng, *Chem. - A Eur. J.*, 2009, **15**, 6504–6517.

44 R. D. Shannon, *Acta Crystallogr. Sect. A*, 1976, **32**, 751–767.

45 K. Matsumoto, R. Hagiwara, Z. Mazej, E. Goreshnik and B. Žemva, *J. Phys. Chem. B*, 2006, **110**, 2138–2141.

46 M. Bolte and H.-W. Lerner, *Acta Crystallogr. Sect. E Struct. Reports Online*, 2001, **57**, m231–m232.

47 I. D. Brown and D. Altermatt, *Acta Crystallogr. Sect. B Struct. Sci.*, 1985, **41**, 244–247.

48 C. Dalvit, C. Invernizzi and A. Vulpetti, *Chem. - A Eur. J.*, 2014, **20**, 11058–11068.

49 S. R. Chaudhari, S. Mogurampelly and N. Suryaprakash, *J. Phys. Chem. B*, 2013, **117**, 1123–1129.

50 J. M. Price, M. W. Crofton and Y. T. Lee, *J. Phys. Chem.*, 1991, **95**, 2182–2195.

51 I. Nahringbauer, S. E. Rasmussen, G. O. Steen, U. Schwieter and J. Paasivirta, *Acta Chem. Scand.*, 1968, **22**, 1141–1158.

52 H. J. Berthold, W. Preibsch and E. Vonholdt, *Angew. Chemie Int. Ed. English*, 1988, **27**, 1524–1525.

53 F. Kraus, S. A. Baer and M. B. Fichtl, *Eur. J. Inorg. Chem.*, 2009, **2009**, 441–447.

54 J. L. Atwood, L. J. Barbour and A. Jerga, *J. Am. Chem. Soc.*, 2002, **124**, 2122–2123.

55 I. Raabe, K. Wagner, K. Guttsche, M. Wang, M. Grätzel, G. Santiso-Quiñones and I. Krossing, *Chem. - A Eur. J.*, 2009, **15**, 1966–1976.

56 M. R. Lacroix, Y. Liu and S. H. Strauss, *Inorg. Chem.*, 2019, **58**, 14900–14911.